Simulation of Drying Stresses in *Eucalyptus nitens* Wood

Natalia Pérez-Peña,[a,*] Cristian Chávez,[b] Carlos Salinas,[c] and Rubén A. Ananías[a]

The objective of this work was to simulate the stresses produced during the drying of *Eucalyptus nitens* wood due to variations in the moisture content. The methodology involved experimental determination and simulation of drying stresses caused by the development of internal moisture content gradients. Modeling of the moisture transport was based on the concept of an effective diffusion coefficient. The mathematical model for stress-strain, and for moisture diffusion into the wood, was constituted by a system of second-order nonlinear partial differential equations with variable coefficients, which were numerically integrated by the control volume based on the finite element method (CVFEM). For validation purposes, tests were realized for evaluating deformations, stress drying, and moisture gradients that were produced during the drying of *Eucalyptus nitens*. The results showed satisfactory agreement between the experimental and simulated values, indicating an effective simulation.

Keywords: CVFEM; Drying modelling; Effective diffusion; Moisture transport; Strains

*Contact information: a: Department of Wood Engineering, Wood Drying Technology & Thermal Treatments Research Group, University of Bío Bío, Av. Collao 1202, 4081112, Concepción, Chile; b: Department of Mechanical Engineering, University of Sao Paulo, Sao Carlos, Brazil; c: Department of Mechanical Engineering, Wood Drying Technology & Thermal Treatments Research Group, University of Bío Bío, Av. Collao 1202, 4081112, Concepción, Chile; *Corresponding author: nattperez@gmail.com*

INTRODUCTION

Mechanical stresses develop within wood when it is exposed to a drying process (Clair 2012). This occurs when the external layers of wood are dried below the fiber saturation point (FSP) and the core is still above the FSP. These stresses are recognized as the main cause of defects and dimensional changes (Larsen and Ormarsson 2013).

To model these stresses, it is necessary to simulate the prior moisture transport into the wood. This allows the moisture gradients that induce dimensional changes and consequently stress and strain to be obtained (Keey *et al.* 2000). To simulate the moisture transport through the wood, diffusive models are typically used for wood dried below the FSP because, above the FSP, the moisture movement occurs by capillarity. However, the model can be used by defining an effective diffusion coefficient (D) that is valid for simulating the drying kinetics of softwoods (Salinas *et al*. 2015) and hardwoods (Sepúlveda *et al*. 2016).

Previous deformation models have mainly focused on the strain caused by the energy (temperature) and mass transport (moisture content). Some authors have proposed one-dimensional models to determine the deformation caused by the heat and mass transport, specifically, the shrinkage and mechano-sorptive strain (Chen *et al*. 1997; Svensson and Martensson 2002; Kang *et al*. 2004; Pang 2007). Additionally, two-dimensional models have been proposed by authors such as Martensson and Svensson

(1997), Perré and Turner (2001a,b), Cheng *et al*. (2007), and Salinas *et al*. (2011a); three dimensional models have been proposed by Ormarsson *et al*. (1999 and 2003), Remond *et al*. (2006), and Hassani *et al*. (2015).

In previous works, beginning with the first studies of McMillen and Youngs (1960) and McMillen (1963) until the present work of Zhan and Avramidis (2017), it was possible to conclude that the stresses and strains produced during wood drying follow a defined pattern. At the beginning of the drying process, the wood surface was dried below the FSP and the core was still above the FSP; this causes shrinkage of the surface layers and produces stress and compresses the core. In the final drying stage, the core loses moisture below the FSP, and this produces reversed stresses; the surface is put under compression, while tensile stresses prevail in the core (Salinas *et al*. 2015).

One difficulty with the simulation of drying stresses is to determine the different types of strain. During the drying process, the total strain (ε) is comprised of shrinkage strain (ε_{fs}), elastic strain (ε_e), mechano-sorptive strain (ε_{ms}), creep strain (ε_c), and temperature-induced strain (ε_T) (Pang 2000; Moutee *et al.* 2007). In this work, the model proposed by Ferguson (1998) was implemented.

Thus, the objective of this work is to simulate the drying stresses in *Eucalyptus nitens* wood as the product of deformation caused by shrinkage and mechano-sorption due to moisture content variations during an isothermal drying process.

EXPERIMENTAL

Materials

The materials consisted of 90 specimens of *Eucalyptus nitens* Deane & Maiden sapwood prepared from the first log of three 12-year-old trees, with a diameter at breast height (DBH) of approximately 34 cm. From each log, one board was cut for the drying test in the radial direction, and other boards for the drying test were cut in the tangential direction. From each board, 15 samples of 25 mm (thickness) × 25 mm (width) × 50 mm (length) were obtained.

Methods

The drying tests were performed in a climate chamber (Binder, KMF-115 model) at a 30 °C dry-bulb temperature, a 25 °C wet-bulb temperature, and 1.5 m/s air velocity. To determine the temperatures inside the chamber, T-type thermocouples connected to a data acquisition system (Fluke, Hidra II model) were used.

The samples were covered with aluminum foil and silicone adhesive so that only the faces of interest were exposed to drying in order to encourage the unidimensional moisture flow in radial or tangential direction.

Three samples were used to monitor the moisture variation in order to obtain the drying curves; these samples were weighed daily using a digital precision balance (A&D GF4000 model). Later, the oven-dry mass was determined by drying in an oven at 103 °C for 24 h. The drying curves were obtained according to,

$$MC = \left[\left(m - m_0 \right) / m_0 \right] * 100 \quad (1)$$

where MC is the moisture content (%), m is the original mass of sample (g), and m_0 is the oven dry mass of sample (g).

Determination of moisture distribution

The remaining samples were used to obtain the spatial distribution of MC. Three samples were removed from the conditioning chamber at 48-h intervals for measurement, weighing and subsequent sectioning in seven slices (thickness about 3 mm) of parallel to the drying surfaces and from one face to other (Fig. 1). The weights were determined with a precision balance (Sartorius, MA 150 model) immediately after cutting and after oven drying at 103 ºC until constant mass to determine the MC distribution according to Eq. (1).

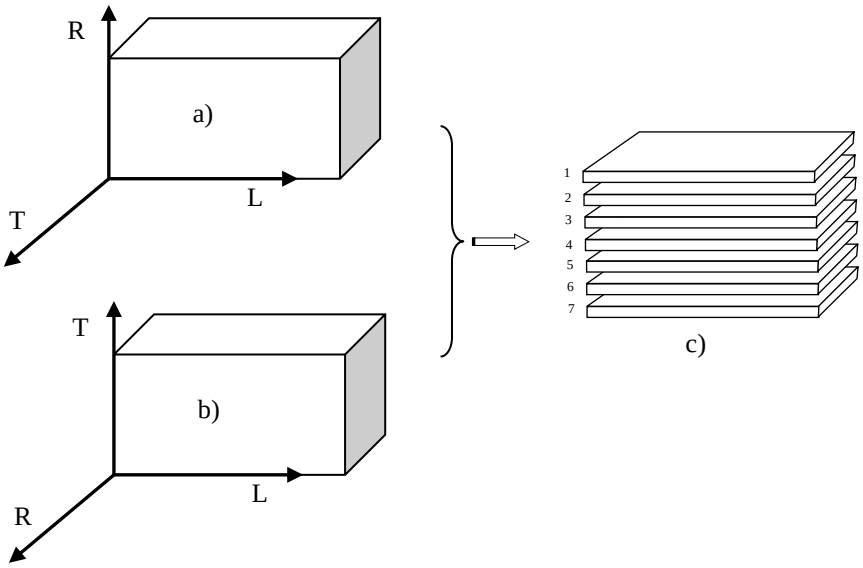

Fig. 1. Cutting scheme and sectioning of samples to radial and tangential moisture distribution for a) radial surfaces, b) tangential surfaces, and c) slices

Strain and stresses

The lengths of each slice were determined with a digital caliper, before and after cutting. The strains were determined as proposed by Morén and Sehlstedt-Persson (1992), based on before drying length (d_g), after drying length (d_d), the length immediately after cutting (d_c) (Fig. 2) and free shrinkage length (d_f).

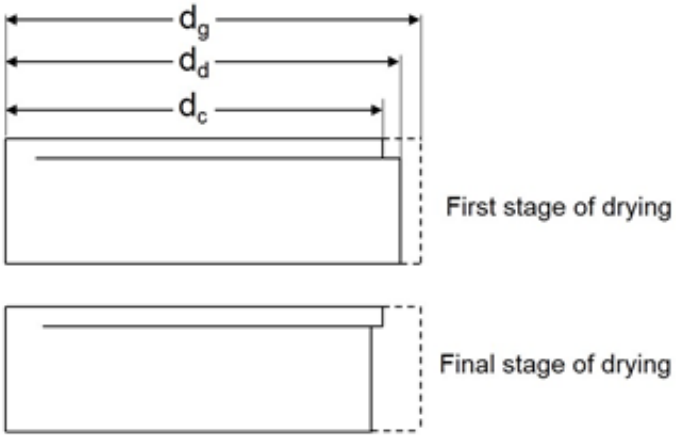

Fig. 2. Scheme of length variation during drying stage

Then, the total strain (ε) was divided in three components: shrinkage (ε_{shrink}), elastic ($\varepsilon_{elastic}$), and creep (ε_{creep}), according to Eq. 2:

$$\varepsilon = \varepsilon_{shrink} + \varepsilon_{elastic} + \varepsilon_{creep} \quad (2)$$

where

$$\varepsilon_{shrink} = \left(d_f - d_g\right)/d_g$$
$$\varepsilon_{elastic} = \left(d_d - d_c\right)/d_g$$
$$\varepsilon_{creep} = \left(d_c - d_f\right)/d_g$$

The stresses (σ) accumulated in the slice and the free shrinkage length (d_f) required by (2) were calculated as proposed by Pang (2000),

$$\sigma = E\left(\frac{d_d - d_c}{d_c}\right)$$
$$d_f = d_g\left(1 - \frac{FSP - MC}{FSP}\beta\right) \quad (3)$$

where E is modulus of elasticity, FSP is the fiber saturation point, Mc moisture content, and β is the shrinkage coefficient.

Simulation

The physical phenomenon of stress and strain was simulated on a cross-section of wood; its properties are presented in Table 1.

The mathematical model for the simulation of MC transport is based on the effective diffusion coefficient and was presented in previous work (Gatica *et al*. 2011). In general terms, the model consists of a second-order nonlinear differential equation that describes the transitory phenomenon of MC diffusion,

$$\frac{\partial MC}{\partial t} = \frac{\partial}{\partial x}\left(D_x \frac{\partial MC}{\partial x}\right) \ (0 < x < L) \quad (4)$$

where MC is moisture content (%), D is effective diffusion coefficient (m^2/s), and L is the samples thickness in the direction of flow (m).

The initial and border conditions were initial moisture $MC=MC_{ini}=90\%$ and convection on surfaces.

D_x was obtained with the following expression:

$$D_x\left(MC\right) = \exp\left(a + bMC\right) \quad (5)$$

The parameters a and b were determined in a previous study (Sepúlveda 2014), through reverse simulation based on experimental drying curves and distribution of MC. The numerical protocol details were explained by Gatica *et al.* (2011).

Table 1. Drying Parameters of *Eucalyptus nitens* Wood

Property	Symbol	Radial	Tangential
*Effective diffusion coefficient	D_x	exp(-22.7+1.3*MC)	exp(-23.1+1.3*MC)
*Convective coefficient (m/s)	h_m	$9.71*10^{-4}$	$7.32*10^{-4}$
**Shrinkage coefficient	A	0.05	0.1
***Mechano sorption coefficient (1/MPa)	M	$1.72*10^{-2}$	$5.3*10^{-2}$
Modulus of elasticity (MPa)	E	2310	1860
Poisson ratio	μ	0.35	
Equilibrium moisture content (%)	EMC	12	
Initial moisture content (%)	MC_{ini}	90	

*Source: Sepúlveda 2014. ** Pérez *et al*. 2016a. ***Pérez *et al*. 2016b.

For the simulation of the stress/strain relationship, the rheological model developed by Ferguson (1998) was implemented with mean mechanical properties for moisture variation below PSF used by Perez *et al.* (2016).

$$\frac{\partial \varepsilon}{\partial t} = \frac{1}{E}\frac{\partial \sigma}{\partial t} + \left(\alpha + m\sigma\right)\frac{\partial MC}{\partial t} \quad (6)$$

In Eq. 6, σ is the stress (Pa), ε is the strain, E is the modulus of elasticity (Pa), α is shrinkage coefficient, and m is mechano sorption coefficient (1/Pa).

This model considers three independent components of strain: elastic (σ/E), free shrinkage $\left(\alpha\Delta MC\right)$ and mechano sorption creep $\left(m\sigma\Delta MC\right)$. Viscoelastic creep was not considered because mechano sorptive creep can be several times greater than the strain obtained under constant moisture content (Langrish 2013).

The model was numerically integrated using the control volume based on the finite element method (CVFEM). The details on the numerical procedure are presented in previous work (Salinas *et al.* 2011a,b).

RESULTS AND DISCUSSION

Drying Curve and Distribution of Moisture

Figure 3 shows the comparison between the approximate experimental and simulated values for the drying curves and the moisture distribution. Drying curves obtained by curve fitting procedure for the radial and tangential directions are shown in Figs. 3a and 3b, respectively. Both the simulated and the approximate values were very similar; the error was lower than 1%, indicating the effectiveness of the model. Since in the model was considered based on an equilibrium MC equal to 12%, it follows that the modeled values of MC cannot be less 12%. On the other hand, the results of curve fitting of experimental values suggested values less than 12%.

Furthermore, for both the radial and tangential directions, the drying curves showed two distinctive stages, starting with an initial stage in which the curve drops rapidly from 85% to 30% of MC. This MC was reached at approximately 160 h in the radial direction and at 224 h in the tangential direction. At this stage, the wood surface is wet, so vaporization begins from there, producing water vapor diffusion through the air/moisture interphase. At the end of this stage, the free water must be transported quickly from the core wood to the surface by capillarity. In the next stage, from approximately 30% to the final MC, bound water begins to move slowly from the core to

the surface, mainly by diffusion. Figures 3c and 3d show the MC profiles for the radial and tangential directions, respectively. The internal profiles are parabolic curves, with minimum values in the outer layers and maximum values in the core.

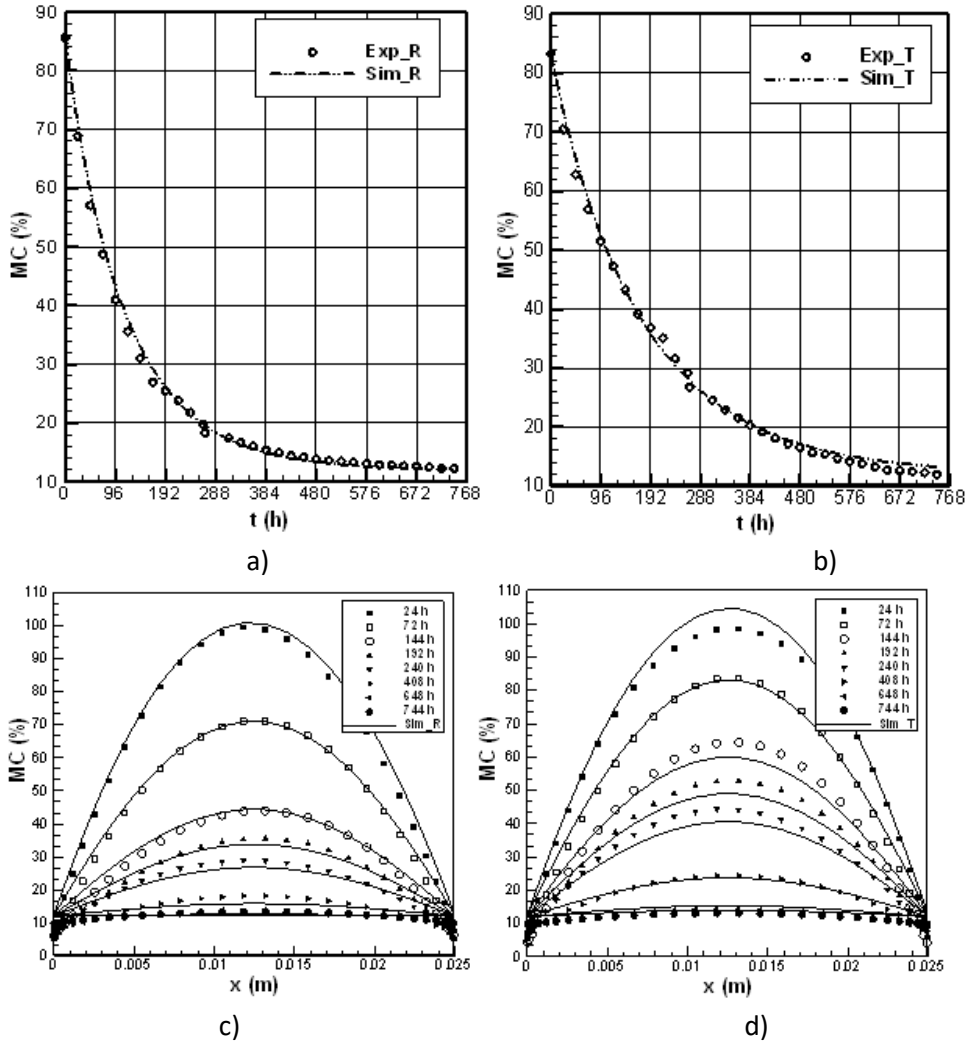

Fig. 3. Drying curve in the (a) radial and (b) tangential directions; MC profiles of the (c) radial and (d) tangential directions.

Strain and stresses

The experimental strain data and MC variation for different drying times are shown in Fig. 4. This figure shows the strain produced at 24, 216, and 720 h of drying in the radial direction (4a, 4c, and 4e) and the tangential direction (4b, 4d, and 4f).

The results confirm that at the beginning of drying (24 h), the outer layers of wood shrink because the MC decreases below the FSP and causes a tensile stress, thus resulting in surface shrinkage ($\varepsilon < 0$) and an extension in the core ($\varepsilon > 0$). At 216 h of drying, the stresses are reversed, the core of the wood shrinks and causes a compressive stress on the surface layers. This produces a negative deformation in the core and a positive deformation in the outer layers. It is at this point that the highest values of deformation are produced, reaching approximately 0.35% in the surface layers and 0.42% in the core in the radial direction, and 0.47% in the surface layers and 0.62% in the core in the tangential direction.

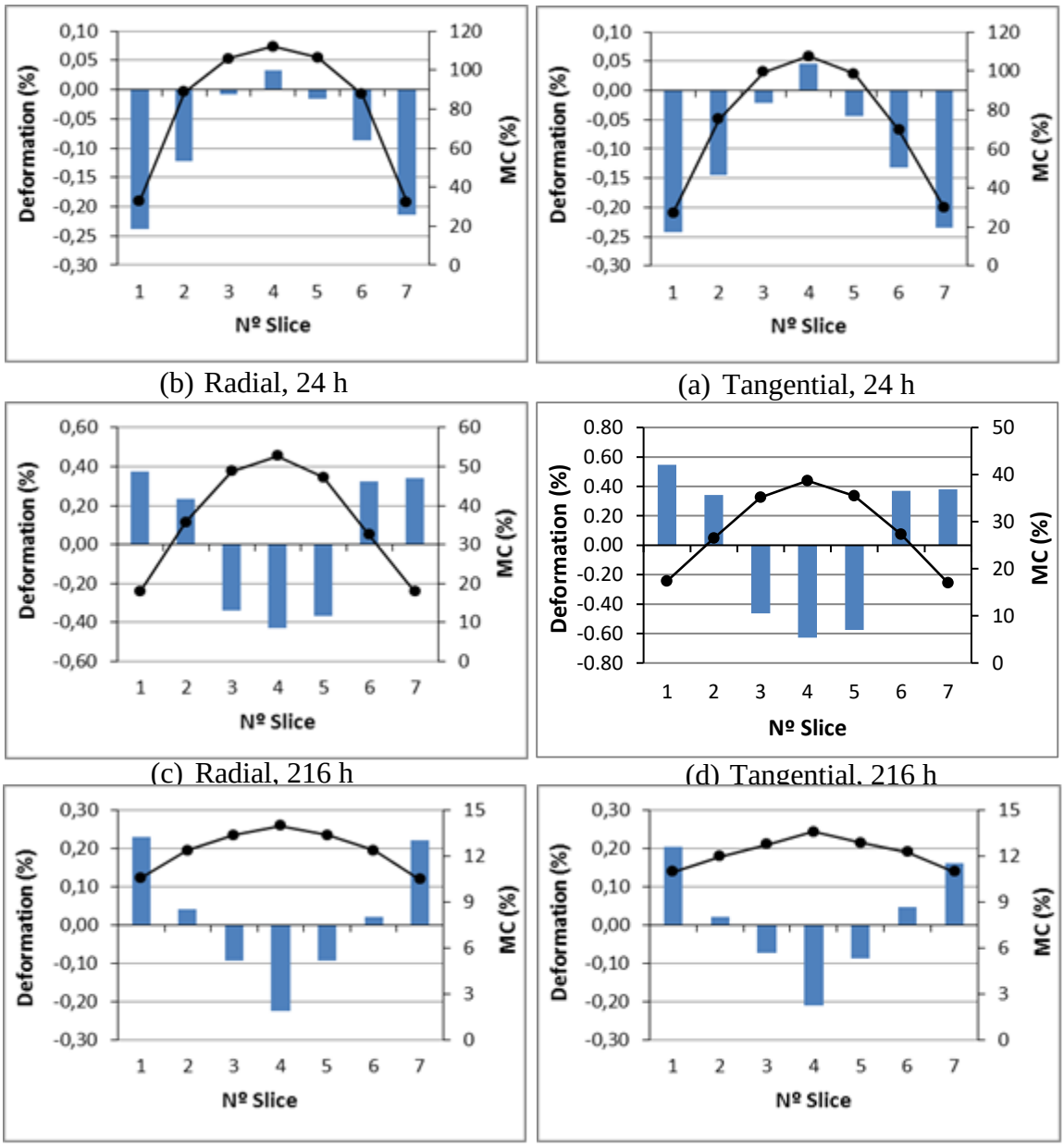

Fig. 4. Experimental strain and MC variation

Furthermore, it is possible to observe that the strain and MC present symmetrical behavior. For example, Fig. 4e shows that the strain in slices 1 and 7 was 0.23% and 0.22%, respectively, and the MC was 10.6% in slice 1 and 10.5% in slice 7.

Figure 5 shows the development of stresses in terms of the drying time for the radial (5a) and tangential (5b) directions. The figures confirm that the outer layers (slice 1 and 7) develop tensile stress in the early stages of drying (approximately 132 h in the radial direction and 144 h in the tangential direction), unlike the core wood (slice 4), which develops a compressive stress. From this moment, the stresses are reversed, and the drying ends with a compressive stress in the surface layers and tension in the core.

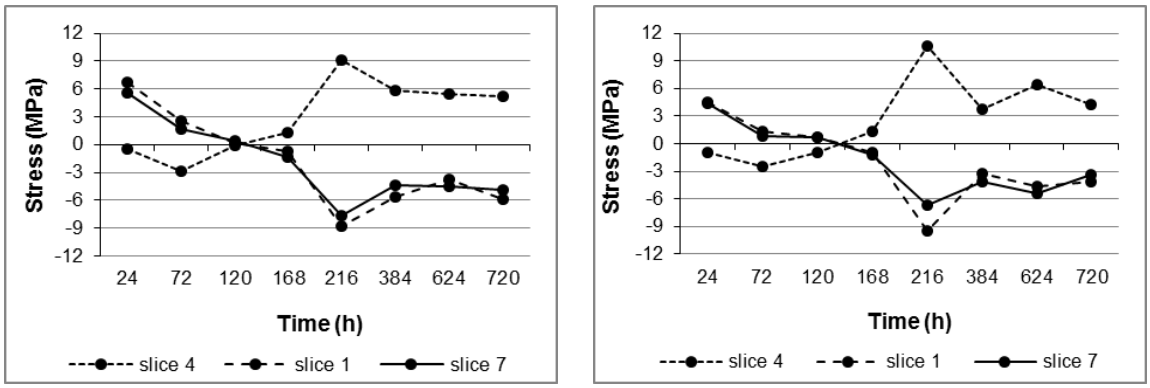

Fig. 5. Evolution of stresses as a function of the drying time in the (a) radial y (b) tangential directions.

The calculated stresses for the radial direction were between 0 and 9 MPa, and for the tangential direction, the values were between 0 and 11 MPa. These values are higher than those reported for *Populus*, with values between 0 and 2 MPa (Salinas *et al*. 2011b), and for radiata pine, with values between 0 and 3 MPa (Salinas *et al*. 2015). Innes (1995) showed values higher than 6 MPa for *E. regnans* regrowth wood of 55 years-old of basic density 673 kg/m^3 and cycles at 20 °C. In previous work with *E. nitens* juvenile wood of 12-years-old, of basic density 488 kg/m^3 (Rebolledo *et al.* 2013) and in which runs were performed at 30 °C, all these factors (juvenile wood, lower density, and higher temperature) increased the drying stresses (Rebolledo *et al.* 2013). Otherwise, the problem of *E. nitens* to produce solid wood is that the extremely highest drying stresses develop during convective drying. Therefore, values of about 10 (MPa) are feasible for a hardwood such as *E. nitens* according to data reported in the literature (Keey *et al.* 2000).

Simulation

Figure 6 shows the results of simulations of stresses for the radial (6a) and tangential directions (6b). In qualitative terms, the stresses showed the expected behavior, indicating the difference between the surface layers and the core wood.

Regarding the magnitudes, it can be seen that for the radial direction, the surface developed a maximum stress of tension of 7 MPa at approximately 40 h. At 140 h, these stresses were reversed, reaching a maximum level of compressive stress of 8 MPa at 400 h. In the core, the maximum compressive stress was approximately -4 MPa and was produced at 100 h. At 160 h, the stresses were reversed, reaching a maximum tensile stress of 3 MPa at 420 h.

In the tangential direction, the surface reached a peak of tensile stress 6.5 MPa at 45 h. These stresses were reversed at 110 h, reaching a maximum compressive stress of -9 MPa at 180 h. In the core, a maximum compressive stress of -4.5 MPa at 100 h was

reached. These stresses were reversed approximately at 120 h, reaching a maximum tensile stress of 3.5 MPa at 360 h.

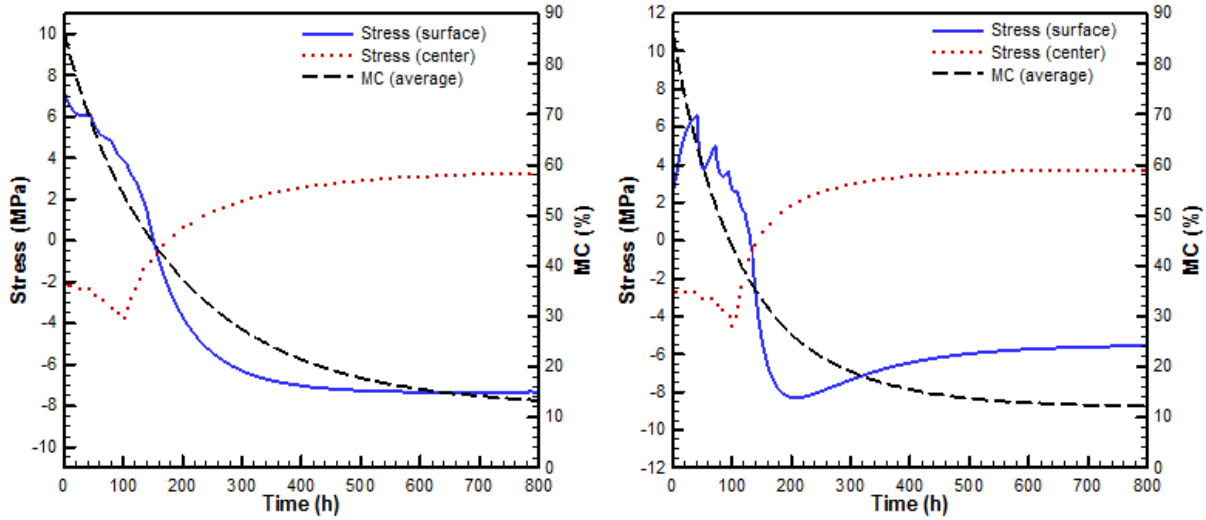

Fig. 6. Simulation of drying stresses in the (a) radial y (b) tangential directions

CONCLUSIONS

1. The behavior of drying stresses during wood drying of *Eucalyptus nitens* is confirmed and can be divided into two distinctive stages: the first drying stage, in which the surface layers develop a tensile stress and compression in the core; and the second drying stage, in which the stresses are reversed, in which the core develops tensile stress and compresses the surface. In the second stage, the highest values are reached: magnitudes of approximately 9 MPa and 11 MPa for the radial and tangential directions, respectively.
2. Regarding the magnitude of the simulated stresses, values for radial stresses are between 0 and 8 MPa, and for tangential stresses, the values are between 0 and 9 MPa.
3. The behavior in the tangential direction of the drying stresses of *E. nitens* support the tendency for surface checks, internal checks and collapse during the drying of solid wood on this anatomical orientation.

ACKNOWLEDGMENTS

The authors are grateful for the financial support from Fondecyt 1160812.

REFERENCES CITED

Chen, G., Keey, R., and Walker, J. (1997). "The drying stress and check development on high-temperature kiln seasoning of sapwood *Pinus radiata* boards. Part I: Moisture movement and strain model," *Holz als Roh-und Werkstoff* 55(2), 59-64. DOI: 10.1007/BF02990517

Cheng, W., Morooka, T., Wu, Q., and Liu, Y. (2007). "Characterization of tangential shrinkage stresses of wood during drying under superheated steam above 100 °C," *Forest Products Journal*, 57(11), 39-43.

Clair, B. (2012). "Evidence that release of internal stress contributes to drying strains of wood," *Holzforschung*, 66(3), 349-353. DOI: 10.1515/hf.2011.159.

Ferguson, W. J. (1998). "The control volume finite element numerical solution technique applied to creep in softwoods," *International Journal of Solid and Structures* 35(13), 1325-1338. DOI: 10.1016/S0020-7683(97)00094-2.

Gatica, Y., Salinas, C., and Ananías, R.A. (2011). Modelling conventional one-dimensional drying of radiata pine based on the effective diffusion coefficient;" *Latin American Applied Research*, 41(2), 183-189.

Hassani, M. M., Wittel, F. K., Hering, S., and Herrmann, H. J. (2015). "Rheological model for wood," *Computer Methods in Applied Mechanical and Engineering* 283, 1032-1060. DOI: 10.1016/j.cma.2014.10.031.

Innes, T. (1995). "Stress model of a wood fiber in relation to collapse," *Wood Sci. Technol.* 29, 363-376. DOI: 10.1007/BF00202584

Kang, W., Lee, N., and Jung, H. (2004). "Simple analytical methods to predict one – and two – dimensional drying stresses and deformations in lumber," *Wood Science and Technology* 38, 417-428. DOI: 10.1007/s00226-004-0230-z.

Keey, R., Langrish, T., and Walker, J. (2000). *Kiln-drying of Lumber*, Springer-Verlag, Berlin, pp. 65-115, 175-181.

Langrish, T. A. G. (2013). "Comparing continuous and cyclic drying schedules for processing hardwood timber: The importance of mechano-sorptive strain," *Drying Technology* 31(10), 1091-1098. DOI: 10.1080/07373937.2013.769449

Larsen, F., and Ormarsson, S. (2013). "Numerical and experimental study of moisture-induced stress and strain field development in timber logs," *Wood Science and Technology* 47(4), 837-852. DOI: 10.1007/s00226-013-0541-z.

Martensson, A., and Svensson S. (1997). "Stress-strain relationship of drying wood – Verification of a one dimensional model and development of a two dimensional model," *Holzforschung* 51(6), 472-478. DOI: 10.1515/hfsg.1997.51.5.472

McMillen, J. (1963). *Stresses in Wood during Drying* (Report Nº 1652), US Department of Agriculture Forest Products Laboratory, Madison, WI.

McMillen, J., and Youngs, R. (1960). *Stresses in Drying Lumber* (Vol. 201, no. 2513) US Department of Agriculture Forest Products Laboratory, Madison, WI.

Morén, T., and Sehlstedt-Persson, M. (1992). "Creep deformation of the surface layer of timber boards during air circulation drying," in: *3rd IUFRO Conference on Wood Drying*, Vienna, pp. 96-102.

Moutee, M., Fortin, Y., and Fafard, M. (2007). "A global rheological model of wood cantilever as applied to wood drying," *Wood Science and Technology* 41, 209-234. DOI: 10.1007/s00226-006-0106-5.

Ormarsson, S., Dahlblom, O., and Petersson, H. (1999). "A numerical study of the shape stability of sawn timber subjected to moisture variation. Part 2: Simulation of drying board," *Wood Science and Technology* 33, 407-423. DOI: 10.1007/BF00702789.

Ormarsson, S., Cown, D., and Dahlblom, O. (2003). "Finite element simulations de moisture related distortion in laminated timber products of norway spruce and radiata pine," in: *8th IUFRO International Wood Drying Conference*. pp. 27-33.

Pang, S. (2000). "Modeling of stress development during drying and relief during steaming in *Pinus radiata* lumber," *Drying Technology* 18(8), 1677-1696. DOI: 10.1080/07373930008917806

Pang, S. (2007). "Mathematical modeling of kiln drying of softwood timber: Model development, validation, and practical application," *Drying Technology* 25(3), 421-431. DOI: 10.1080/07373930601183751

Pérez, N., Cloutier, A., Segovia, F., Salinas, C., Sepúlveda, V., Salvo, L., Elustondo, D., and Ananías, R. A. (2016a). "Hygromechanical strains during the drying of *Eucalyptus nitens* boards," *Maderas-Ciencia y Tecnología* 18(2), 235-244. DOI: 10.4067/S0718-221X2016005000021.

Pérez, N., Segovia, F., Salinas, C., and Ananías, R. A. (2016b). "Perpendicular mechano-sorptive strains during moisture desorption from *Eucalyptus nitens* specimens," *BioResources* 11(4), 8277-8284. DOI:10.15376/biores.11.4.8277-8284.

Perré, P., and Turner, I. (2001a). "Determination of the material property variations across the growth ring of softwood for use in a heterogeneous drying model. Part I. Capillary pressure, tracheid model and absolute permeability," *Holzforschung* 55(3), 318-323. DOI: 10.1515/HF.2001.052

Perré, P., and Turner, I. (2001b). "Determination of the material property variations across the growth ring of softwood for use in a heterogeneous drying model. Part II. Use of homogenization to predict bound liquid diffusivity and thermal conductivity," *Holzforschung* 55(4), 417-425. DOI: 10.1515/HF.2001.069

Rebolledo, P., Salvo, L., Contreras, H., Cloutier, A., and Ananías, R. A. (2013). "Variation of internal checks related with anatomical structure and density in *Eucalyptus nitens* wood," *Wood and Fiber Science* 45(3), 279-286.

Remond, R., Passard, J., and Perré, P. (2006). "The effect of temperature and moisture content on the mechanical behavior of wood: a compressive model applied to drying and bending," *European Journal of Mechanical Solid* 26, 558-575. DOI: 10.1016/j.euromechsol.2006.09.008.

Salinas, C., Chávez, C., Gatica, Y., and Ananías, R. (2011a). "Two-dimensional wood drying stress simulation using control-volume mixed finite element methods (CVFEM)," *Ingeniería e Investigación* 31(1), 171-183.

Salinas, C., Chávez, C., Gatica, Y., and Ananías, R. (2011b). "Simulation of wood drying stresses using CVFEM," *Latin American Applied Research* 41, 23-30.

Salinas, C., Chávez, C., Ananías, R., Elustondo, D. (2015). "Unidimensional simulation of drying stress in radiata pine wood," *Drying Technology* 33(8), 996-1005. DOI: 10.1080/07373937.2015.1012767.

Sepúlveda, V. (2014). *Simulación de la Cinética del Secado a Baja Temperatura de Eucalyptus nitens*, Master´s Thesis, University of Bío Bío, Concepción, Chile.

Sepúlveda, V., Pérez, N., Salinas, C., Salvo, L., Elustondo, D., and Ananías, R. (2016). "The development of moisture and strain profiles during predrying of *Eucalyptus nitens*," *Drying Technology* 34(4), 428-436. DOI: 10.1080/07373937.2015.1060490.

Svensson, S., and Martensson, A. (2002). "Simulation of drying stresses in wood. Part II: Convective air drying of sawn timber," *Holz als Roh- und Werkstoff* 60, 72-80. DOI: 10.1007/s00107-001-0266-9.

Zhan, J. F., and Avramedis, S. (2017). "Evaluation strategy of softwood drying stresses during conventional drying: A 'mechano-sorptive creep gradient' concept," *Wood Sci. Technol.* DOI 10.1007/s00226-017-0937-2.

Article submitted: December 28, 2016; Peer review completed: March 17, 2017; Revised version received: December 24, 2017; Accepted: December 27, 2017; Published: January 8, 2018.
DOI: 10.15376/biores.13.1.1413-1424